journal of the mechanical behavior of biomedical materials 146 (2023) 106096

Contents lists available at ScienceDirect

Journal of the Mechanical Behavior of Biomedical Materials

journal homepage: www.elsevier.com/locate/jmbbm

Effect of preparation design on fracture strength of compromised molars restored with lithium disilicate inlay and overlay restorations: An in vitro and in silico study

Jelte W. Hofsteenge [a,*], Marco Aurelio Carvalho [b], Pauline M. Borghans [a], Marco S. Cune [a,c], Mutlu Özcan [a,d], Pascal Magne [e], Marco M.M. Gresnigt [a,f]

[a] University of Groningen, University Medical Center Groningen, Center for Dentistry and Oral Hygiene, Department of Restorative Dentistry, Groningen, the Netherlands
[b] Dental School, Evangelical University of Goias, Anapolis, Brazil
[c] St. Antonius Hospital Nieuwegein, Department of Oral-Maxillofacial Surgery, Prosthodontics and Special Dental Care, Nieuwegein, the Netherlands
[d] University of Zurich, Center of Dental Medicine, Division of Dental Biomaterials, Clinic for Reconstructive Dentistry, Zurich, Switzerland
[e] Center for Education and Research in Biomimetic Restorative Dentistry (CER BRD), Beverly Hills, CA, USA
[f] Martini Hospital, Department of Special Dental Care, Groningen, the Netherlands

ARTICLE INFO

Keywords:
Adhesion
Ceramic
Dental materials
Fracture strength
Cusp coverage
Lithium disilicate
Inlay
Overlay
Failure mode
Fatigue
Adhesive dentistry
FEA

ABSTRACT

Purpose: The objective of this study was to determine the influence of different preparation designs on the fracture strength, failure type, repairability, formation of polymerization-induced cracks, and tooth deformation of structurally compromised molars restored with lithium disilicate inlays and overlays in combination with Immediate Dentin Sealing (IDS).

Material and methods: Human molars (N = 64) were randomly assigned to four different preparation designs: Undermined Inlay (UI), Extended Inlay (EI), Restricted Overlay (RO), and Extended Overlay (EO). The teeth were restored using lithium disilicate partial restorations and subjected to thermomechanical fatigue in a chewing simulator (1,2 × 10 (Mondelli et al., 2007) cycles on 50 N, 8000x 5–55 °C), followed by load to failure testing. In silico finite element analysis was conducted to assess tooth deformation. Polymerization-induced cracks were evaluated using optical microscopy and transillumination. Fracture strengths were statistically analyzed using a Kruskal-Wallis test, while the failure mode, repairability, and polymerization cracks were analyzed using Fisher exact test.

Results: The propagation of polymerization-induced cracks did not significantly differ among preparation designs. All specimens withstood chewing simulator fatigue, with no visible cracks in teeth or restorations. Fracture strength was significantly influenced by preparation design, with restricted overlay (RO) showing higher fracture strength compared to extended inlay (EI) ($p = .042$). Tooth deformation and fracture resistance correlated between in vitro and in silico analyses). UI exhibited a statistically less destructive failure pattern than EO ($p < .01$) and RO ($p = .036$). No statistically significant influence of the preparation design on repairability was observed. Groups with higher repairability rates experienced increased tooth deformation, leading to less catastrophic failures.

Conclusions: The preparation design affected the fracture strength of compromised molars restored with lithium disilicate inlays and overlays, with significantly lower fracture strength for an extended inlay. The failure pattern of lithium disilicate overlays is significantly more destructive than that of undermined and extended inlays. The finite element analysis showed more tooth deformation in the inlay restorations, with lower forces in the roots, leading to less destructive fractures. Since cusp coverage restorations fracture in a more destructive manner, this study suggests the undermined inlay preparation design as a viable option for restoring weakened cusps.

* Corresponding author. University of Groningen, University Medical Center Groningen, Department of Restorative Dentistry, Center for Dentistry and Oral Hygiene, Antonius Deusinglaan 1, 9713 AV, Groningen, the Netherlands.
E-mail address: j.w.hofsteenge@umcg.nl (J.W. Hofsteenge).

https://doi.org/10.1016/j.jmbbm.2023.106096
Received 8 June 2023; Received in revised form 24 August 2023; Accepted 28 August 2023
Available online 28 August 2023

1. Introduction

Structurally compromised teeth can be restored using direct or indirect restorations. The advantages of an indirect restoration include the ease of achieving proper approximal contour, occlusal morphology, and marginal adaptation (Manhart et al., 2004). In addition, there is less shrinkage during polymerization, reducing the risk of crack formation and microleakage (Dejak and Młotkowski, 2015). Disadvantages of an indirect restoration are that it is more time-consuming, expensive, and potentially involves more loss of sound tissue than a direct restoration, as divergence of walls is required for an indirect restoration (Kuijs et al., 2006).

In the past, posterior restorations were often made of amalgam. Amalgam restorations relied on convergent preparations for macro-mechanical retention. Removing an amalgam restoration renders tooth structure undermined, and the need for coverage of the cusps has been suggested to be good clinical practice. Although little scientific evidence exists regarding minimum wall thickness, cusp coverage is recommended in some articles to prevent fracturing of the affected tooth at a wall thickness smaller than 2-2,5 mm (Rocca et al., 2015; Politano et al., 2018).

Since the fracture strength of a tooth is partly dependent on the amount of remaining tooth material, it is still unclear to what extent the fracture strength is affected by different preparation designs (Mondelli et al., 2007). Yamanel et al. observed in a finite element analysis that an onlay protected the remaining tooth better than an inlay (Yamanel et al., 2009). However, there is still ambiguity regarding the effect of the cusp coverage on the fracture strength of the restored teeth (Yoon et al., 2019; Hofsteenge et al., 2020, 2021; Bresser et al., 2020; Alassar et al., 2021). The meta-analysis in a systematic review on the fracture strength of inlay, onlays and overlays reported no statistical significant differences in fracture strength between inlays and onlays and between inlays and overlays (Amesti-Garaizabal et al., 2019). Teeth should be prepared minimally invasively, but on the other hand restorative material requires a certain minimal thickness for sufficient strength and clinical management (Politano et al., 2018).

One disadvantage of cusp coverage restorations is that more sound tooth tissue is removed than without cusp coverage (Rocca et al., 2015). Additionally, in vitro studies demonstrate that overlays are more likely to fracture in an unfavorable manner, specifically apical to the enamel-cement interface, which challenges the repairability of the tooth (Hofsteenge et al., 2020; Bresser et al., 2020). However, a literature review that included *in vivo* studies shows that an onlay appears to be a good way to restore posterior teeth and that the most common fracture occurs in the ceramic restorative material (Abduo and Sambrook, 2018).

Since extensive replacement restorations expose dentin, it is recommended to seal the freshly prepared dentin with bonding for improved adhesion (Qanungo et al., 2016; van den Breemer et al., 2017). This is called Immediate Dentin Sealing (IDS). The majority of studies on fracture strength in cusp coverage did not include IDS, while it appears that the use of IDS generally provides higher fracture strength of restored molars (Hofsteenge et al., 2020).

The influence of the preparation design in combination with IDS on fracture strength has not yet been studied extensively. For this reason, the objective of this in vitro study is to study the influence of different preparation designs on the fracture strength, failure type, repairability, and formation and propagation of polymerization-induced cracks of compromised molars restored with lithium disilicate inlays and overlays in combination with IDS. The null hypotheses tested were that 1) there is no difference in formation and propagation of microcracks; 2) there would be no effect of preparation design on the fracture strength; there is no difference in 3) failure mode and 4) repairability in vitro and 5) there is no difference in silico on tooth deformation between the preparation designs.

2. Material and methods

The brands, types, manufacturers, chemical compositions, and batch numbers of the materials used in this study are listed in Table 1.

2.1. Selection and randomization

Sound human molars (N = 64), were selected from a pool of recently extracted teeth (<6 months, conserved in water). The molars were divided into three groups of similar size (small, medium, large) based on coronal dimensions. The teeth were than randomly distributed from each size group into the four research groups. Approval of the ethical committee was not required, as stated in a IRB-statement. To detect differences in fracture strength, the sample size was based on the following parameters and assumptions: effect size 0.45, $\alpha = 0.05$, Power = 0.8, and the number of groups = 4 (Faul et al., 2007). The effect size was set based on the results from previous studies (Hofsteenge et al., 2020, 2021).

All procedures were performed by one operator. The teeth were embedded in polymethylmethacrylate (Probase Cold, Ivoclar Vivadent, Schaan, Liechtenstein) up to 1 mm below the cement-enamel junction (CEJ). Photographs were made of each specimen. Specimens were stored in water during the time of the study. Teeth were then randomly assigned to one of four groups. Fig. 1 shows the experimental sequence, allocation, and abbreviations of the groups.

2.2. Specimen preparation

Prior to preparation, a relined putty index (Provil Novo, Kulzer & Fit Checker Advanced, GC Corporation, Tokyo, Japan) was made for the purpose of temporary provision. In addition, a digital scan of the original tooth was made using an intra-oral scanner (CEREC Omnicam, software CEREC SW 5.2.1, Dentsply Sirona, Charlotte, NC, USA) for restoring the original morphology in the final restoration.

Four experimental preparation design groups were made on the teeth (Fig. 2).

- Undermined inlay (UI): The preparation width was 70% of the intercuspal width. The depth was 5 mm relative to the highest cusp and the width of the approximal box was 5 mm. The walls were prepared straight after which an undercut was made in the dentin (using round diamond burs). To do this, the thickness of the cusps was first measured with a thickness gauge, then the cusp was undermined by 1 mm.
- Extended inlay (EI): The preparation width was 100% of the intercuspal width, without undermining. Walls were prepared with 6° divergency. The depth was 5 mm relative to the highest cusp and the width of the approximal box was 5 mm.
- Restricted overlay (RO): First, the preparation of the 100% inlay was made, then the cusps were lowered by 1.5 mm. The preparation on the reduced cusps ends obliquely upward at an angle of 20°.
- Extended overlay (EO): First, the preparation of the 100% inlay was made, thereafter the cusps were lowered by 4 mm. The preparation ends obliquely downward at an angle of 10°.

The preparations were performed under 10× microscope magnification (OPMI Pico, Zeiss, Oberkochen, Germany). Preparation was made with coarse diamond chamfer burs (6847 KR, Komet Dental, Lemgo, Germany) and fine diamond chamfer burs (8847 KR & 8856, Komet Dental). The entire preparation was finished smoothly with a Brownie (9609, Komet Dental) and Greenie (9620, Komet Dental). Water cooling was used during preparation. A bevel of 0.5 mm width was applied to all approximal boxes using a sonic handpiece (Sonicflex, Kavo Dental, Biberach an der Riβ, Germany).

Immediately after preparation, IDS was applied. The dentin was etched for 15 s with 35% phosphoric acid (Ultra-etch, Ultradent, South

Table 1
The brands, types, chemical compositions, manufacturers and batch numbers of the main materials used in this study.

Product Name	Type	Chemical composition	Manufacturer	Batch number
Ultra-etch	Etch gel	35% phosphoric acid	Ultradent Products. Inc, South Jordan, UT, USA	BKRHZ, BJMTY
Optibond FL Prime	Primer	HEMA, GPDM, MMEP, ethanol, water, initiators	Kerr, Orange, CA, USA	8272741
Optibond FL Adhesive	Bonding agent	Bis-GMA, HEMA, GPDM, barium-aluminum borosilicate glass, disodium hexafluorosilicate, fumed silica	Kerr, Orange, CA, USA	7318375, 8503590
Tetric Evo Flow	Flowable composite	dimethacrylates (38 % wt), barium glass, ytterbium trifluoride, highly dispersed silicon dioxide, mixed oxide and copolymer (62 % wt). Additives, catalysts, stabilizers and pigments (<1 % wt).	Ivoclar Vivadent, Schaan, Liechtenstein	Z01MBK
K–Y gel	Glycerin gel	Purified water, Glycerin, Methylparaben, Propylparaben, Propylene Glycol, Hydroxyethylcellulose, Dissodium, Phosphate, Sodiumphosphate, Tetrasodium, EDTA	Johnson & Johnson, New Brunswick, NJ, USA	B213520
Durelon powder	Carboxylate cement	Zinc oxide, stannous fluoride, tin dioxide	3M Espe, St Paul, MN, USA	4788355
Durelon liquid	Carboxylate cement	Water, polyacrylic acid	3M Espe, St Paul, MN, USA	593814
Cojet Sand	Silica-Coating Agent 30 μm	Aluminum trioxide particles coated with silica	3M ESPE, St Paul, MN, USA	8644196
Bis Silane	Silane coupling agent	Ethanol, 3-(trimethoxysilyl)propyl-2-methyl-2-propenoic acid	Bisco, Schaumburg, IL, USA)	2100000581
Porcelain etch	Etching gel	Hydrofluoric acid (9%)	Ultradent Products. Inc, South Jordan, UT, USA	BKCPD
IPS ceramic Neutralizing Powder	Neutralization powder	25–50% sodium cabonate, 25–50% calcium carbonate	Ivoclar Vivadent, Schaan, Liechtenstein	Z01TBZ
Enamel Plus HFO	Micro-hybrid light-cured composite	Diurethandimethacrylate, Bis-GMA, 1,4-Butandioldimethacrylate. glass filler: highly dispersed silicone dioxide	Micerium, Avegno, Italy	2021008814
IPS e.max CAD	Lithium disilicate blocks	SiO2, Li2O, K2O, MgO, ZnO, Al2O3, P2O5 and other oxides.	Ivoclar Vivadent, Schaan, Liechtenstein	Z01RMM, Z020B4
IPS e.max CAD glaze	Glaze paste		Ivoclar Vivadent, Schaan, Liechtenstein	Z01ZMX

The full names of the abbreviations: HEMA: 2-Hydroxyethyl methacrylate, Bis-GMA: Bisphenol A diglycidyl ether dimethacrylate, GPDM: Glycidyl methacrylate propyl dimethacrylate, MMEP: Methyl methacrylate ethylene glycol dimethacrylate phosphate, EDTA: Ethylenediaminetetraacetic acid.

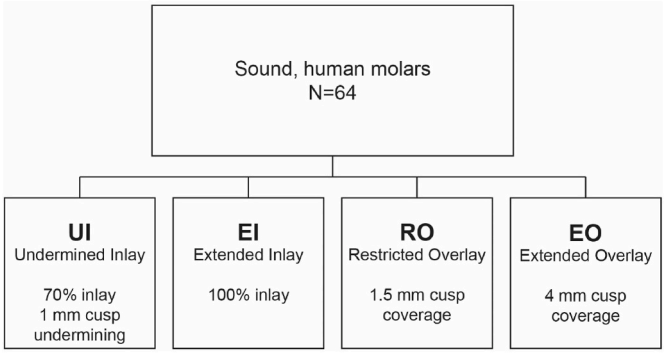

Fig. 1. Flow-chart showing experimental sequence, allocation, and abbreviation of the groups. UI = undermined inlay, EI = extended inlay, RO = restricted overlay, EO = extended overlay.

Jordan, Utah, USA), rinsed thoroughly with water for 15 s, and air dried for 5 s. The primer (Optibond FL Prime, Kerr, Orange, CA, USA) was applied by active rubbing for 20 s. Primer excess was removed by using a combination of air-drying with suction to remove the evaporated solvent. Adhesive (Optibond FL Bond, Kerr) was applied for 15 s, air-thinned, and photo-polymerized for 20 s in close proximity of the restoration using an LED polymerization lamp (Bluephase 20i, wave length range 385–515 nm, light tip diameter 8 mm Ivoclar Vivadent). Prior to polymerization, the output of the polymerization device was verified to be at least 1200 mW/cm^2 (Bluephasemeter II; Ivoclar Vivadent). A thin layer of flowable composite (Tetric Evoflow, Ivoclar Vivadent) was applied and spread with a probe and photo-polymerized for 40 s. The undermining of cusps in the UI group was filled with flowable composite. Next, glycerin gel (K–Y Lubricating Jelly, Johnson & Johnson, New Brunswick, NJ, USA) was applied over the IDS layer, exposed for 40 s to photo-polymerize the oxygen inhibition layer, and rinsed away with water. The excess on the enamel was removed with a fine diamond bur (8856, Komet Dental). The IDS layer was polished with a Brownie (9609, Komet Dental).

2.3. Digital impression and temporary restoration

After preparation, the scan made prior to preparation was retrieved on the CEREC Omnicam, then the preparation was scanned. The intra-oral scanner was calibrated each time it was used. A temporary provision (Protemp 4, 3M ESPE, St Paul, MN, USA) was made using the putty index. The temporary restoration was finished with abrasive discs (Soflex, 3M ESPE) and cemented with temporary cement (Durelon, 3M ESPE). The specimens were stored in water at room temperature for three weeks.

2.4. Fabrication of the restorations

The biogeneric digital copy of the original tooth can be used for the fabrication of the restorations. All restorations were made of lithium disilicate (IPS e.max CAD, High Translucency, A3, Ivoclar Vivadent). The lithium disilicate restorations were milled using a milling unit (MC-XL, Dentsply Sirona). After crystallization and glazing (IPS e.max CAD Crystallization Glaze Paste FLUO, Ivoclar Vivadent) in a ceramic furnace (Programat, Ivoclar, Vivadent), the intaglio of the restorations was checked for excess glaze paste, and if present, it was removed.

2.5. Adhesive placement of the restorations

The final restorations were luted with heated resin composite (Enamel Plus HFO UD3 (A3), Micerium, Avegno, Italy). First, the temporary provision was removed with a scaler. The specimen was cleaned with a polishing brush and pumice and thoroughly rinsed with water. The fit of the final restorations was checked using a probe. The IDS layer was tribochemically conditioned (Cojet Sand, 3M ESPE) for 2–3 s at 2

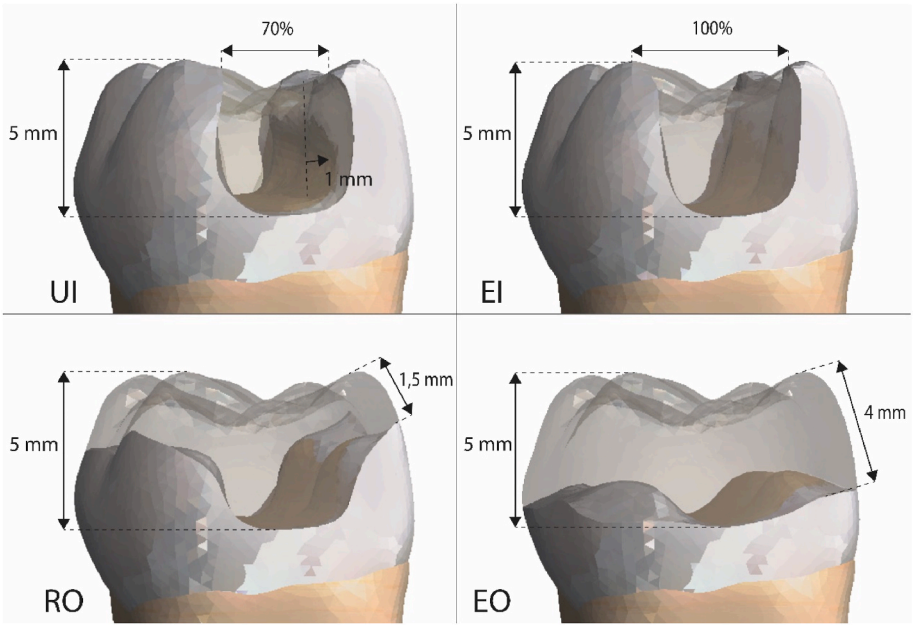

Fig. 2. Schematic visualization of the experimental preparation groups. UI: undermined inlay; EI: extended inlay; RO: restricted overlay; EO: extended overlay.

bars until the surface becomes dull. The specimens were rinsed with water and air-dried. The enamel was etched for 30 s with 35% phosphoric acid (Ultra-etch, Ultradent), rinsed thoroughly with water for 15 s, and air-dried. Silane (Bis-Silane, Bisco, Schaumburg, IL, USA) was applied to the IDS layer and allowed to dry for 5 min (Rita et al., 2021). Meanwhile, the intaglio of the restoration was first treated with hydrofluoric acid (9% porcelain etch, Ultradent) for 60 s, thoroughly rinsed for 15 s in water with neutralizing powder (IPS Ceramic neutralizing powder, Ivoclar Vivadent) and air-dried, after which it should have a dull white appearance. Thereafter it was etched with 35% phosphoric acid (Ultra-etch, Ultradent) for 60 s in a rubbing motion. The restoration was cleaned in an ultrasonic cleaning bath (Emmi 4, EMAG, Mörfelden-Walldorf, Germany) with demineralized water for 5 min and air-dried. Silane (Bis-silane, Bisco) was applied to the restoration, after which it was dried for 5 min at 100 °C (D1500, Coltene, Altstätten, Switzerland). Just before luting, adhesive (Optibond FL Bond, Kerr) was applied to the entire preparation and the intaglio of the restoration. This was air-dried until no movement was visible. The adhesive was not polymerized. Resin composite (Enamel Plus HFO) was pre-heated to 63 °C (Ease-It, Ronvig, Daugaard, Denmark) and applied to the preparation. The restoration was placed under constant pressure and excess of the luting composite was removed with a probe and microbrush. Once placed, glycerin gel (K–Y lubricating jelly, Johnson & Johnson) was applied all around and photo-polymerized from each side with the same LED polymerization device for 80 s. The margins were finished using fine diamond burs (Komet Dental), EVA handpiece (Kavo) and brownies (Komet Dental).

2.6. Transillumination

In order to detect stress-induced polymerization cracks, specimens were evaluated two times during this study at 1.5 × magnification (Canon EOS 70D with a Canon 100 mm macro lens with Macro Ring Lite flash) under standardized conditions and with transillumination (Microlux, Addent, Cupertino, CA, USA): before preparation and one week after restoration. Transillumination before preparation revealed pre-existing cracks. Cracks were categorized on a three-level classification: (a) no cracks visible, (b) visible cracks smaller than 3 mm, and (c) visible cracks larger than 3 mm.

2.7. Thermomechanical fatigue, fracture test and analysis

All specimens were subjected to fatigue loading within a chewing simulator (SD Mechatronik CS-4.8 Chewing Simulator, Feldkirchen-Westerham, Germany) utilizing a zirconia ceramic antagonist sphere loaded on the occlusal plane for 1.2×10^6 cycles (1.7 Hz, 50 N). Simultaneously, they were thermocyclic aged for 8000 cycles (ranging between 5 and 55 °C). After the fatigue, the specimens were evaluated on failures and fractures using magnification (40x, Wild, Heerbrugg, Switzerland) and digital pictures were made. Subsequently, the specimens were mounted in the Universal Testing Machine (810 Material Test System, MTS, Eden Prairie, USA) and subjected to loading with an 8 mm steel ball, positioned on the buccal cusp under an angle of 30° to the tooth axis, with a crosshead speed of 1 mm/min. The maximum load before failure (N) was documented. Failures were initially observed using an optical microscope (40x, Wild) and categorized using the following classifications: 1) fracture of enamel; 2) fracture of enamel and dentin; 3) fracture of the restoration; 4) fracture of the restoration and enamel; 5) fracture of the restoration, enamel and dentin; 6) root fracture. Fractures above the CEJ were additionally classified as 'repairable', while those that were situated below the CEJ and extended in the root were categorized as 'non-repairable'.

Data were analyzed using a statistical software package (SPSS 28, SPSS inc., Chicago, USA). Kolmogorov-Smirnov tests were used to test normal distribution of the fracture strength data. As these data were not normally distributed ($p < .05$), a Kruskal-Wallis test was applied to analyze the effect of the preparation design on the fracture strength, post hoc comparisons (with Bonferroni correction) were applied to analyze differences between groups. The failure mode and repairability data were analyzed with a Fisher exact test with post hoc test with Bonferroni correction as the assumptions for Chi-square were violated. For all tests, a significance level of 0.05 has been used.

2.8. In silico analysis

A three dimensional (3D) finite element analysis was performed considering the same study factors and specimen designs used in the in vitro test, in order to better understand the biomechanical behavior of different models.

A human lower left first molar was used for 3D FEA models

generation. The intact molar was firstly used to obtain separated surfaces of enamel, dentin and pulp chamber by CBCT scan, was obtained DICOM files were treated and exported as STL files according to a previously described process (Camargos et al., 2020) in a specific software (InVesalius, Renato Archer Information and Technology Center, Campinas, Brazil). First, the intact tooth surface was then scanned with an intraoral scanner (CEREC Omnicam, Dentsply Sirona, software CEREC SW 5.2.1). Within the same tooth, all preparations were made in scanned in the following sequence to obtain the most corresponding preparations: scans of the preparation of the undermined inlay, the extended inlay, the restricted overlay, and the extended overlay preparation were made. The STL files obtained from the CBCT scan and iOS scans were combined in open-source software (Meshmixer, Autodesk Inc.) for mesh refinement prior to being exported to CAD software (SolidWorks, 2018, Dassault Systèmes, SolidWorks Corporation, Concord, MA, USA), where final four models were generated in accordance to the in vitro specimens: undermined inlay (UI), extended inlay (EI), restricted overlay (RO) and extended overlay (EO).

The four CAD models were exported to specific software (ANSYS Workbench 14, Ansys Inc., Canonsburg, Pennsylvania, USA) for numerical analysis. The properties of the material used in the models were obtained in the literature and are presented in Table 2 (Lin et al., 2008; Trindade et al., 2018; Ausiello et al., 2019; Park and Choi, 2017). All the materials were considered linearly elastic, homogenous, and isotropic.

The mesh was generated by using quadratic tetrahedral elements. After the 5% convergence analysis (Lan et al., 2010), a 0.3 mm element size was set. Contacts between parts of the model were defined to be bonded. The boundary conditions were defined by fixing the lateral and lower surfaces of the acrylic base in all directions. In order to simulate the loading condition performed in the in vitro test, a 30° oblique load was applied to the buccal cusp. A 131.9 N was chosen in order to simulate clinical condition of mean bite force (Rodrigues et al., 2020).

The deformation values were obtained for quantitative analysis. Color-coded scales were used for tooth deformation in the qualitative analysis.

3. Results

Considering the formation of polymerization-shrinkage induced cracks, The Fisher exact test reported no statistically significant influence of the preparation design on an increase in microcracks ($p > .05$). Fig. 3 shows the distribution of the size of microcracks for the four preparation designs after preparation and 1 week after restoration.

All specimens withstood the fatigue loading in the chewing simulator, no visible fractures were observed in the tooth or the restoration. One of the specimens fractured during incorrect removal from the chewing simulator, one specimen fractured during load to failure at the apex of the molar, both specimens were excluded from analysis. Descriptive analysis of fracture strengths and in silico tooth deformation are shown in Table 3. Fracture strength of the groups was not normally distributed, as shown by the Kolmogorov-Smirnov test for normality ($p < .02$). A Kruskal-Wallis test with post hoc comparisons was conducted

Table 2
Material properties used in this study.

Material	Elastic Modulus (GPa)	Poisson's ration
Dentin (Lin et al., 2008)	18.6	0.31
Enamel (Lin et al., 2008)	84.1	0.30
Pulp (Lin et al., 2008)	0.002	0.45
IPS e.max CAD, Ivoclar vivadent (Trindade et al., 2018)	83.5	0.21
Tetric Evoflow, Ivoclar Vivadent (Ausiello et al., 2019)	8.0	0.2
Acrylic Resin (Park and Choi, 2017)	3.2	0.3

Superscript numbers refer to references.

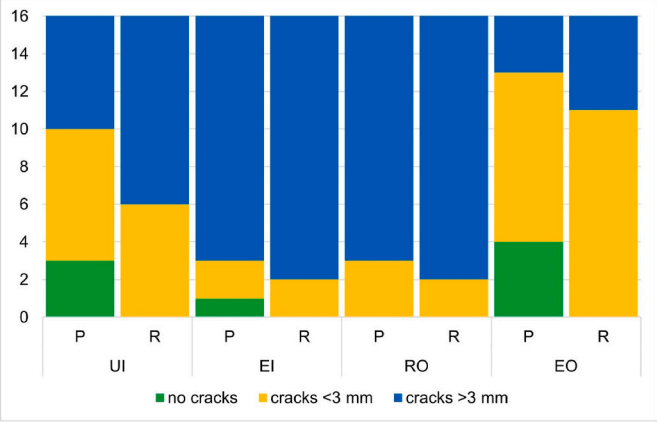

Fig. 3. Distribution of micro-cracks after preparation (P) and 1 week after restoration (R). UI: undermined inlay, EI: extended inlay, RO: restricted overlay, EO: extended overlay.

to examine the influence of preparation design on the fracture strength. There was a statistically significant influence of the preparation design on fracture strength ($p = .046$). Pairwise comparisons revealed a statistically significant higher fracture strength in RO in comparison with EI ($U = 53$, $p = .042$).

A Fisher exact test revealed a significant interaction between the preparation design and the failure mode ($p < .001$). UI exhibited a different failure pattern than EO ($p < .01$) and RO ($p = .036$). Fig. 4 illustrates the distribution of failure modes among the groups. Fig. 5 visualizes representative examples of the modes of failure. No significant correlation was observed between the preparation design and the repairability of the specimens ($p > .05$). Fig. 6 visualizes the repairability of the groups.

There might be a correlation between the in vitro fracture resistance and in silico tooth deformation. Groups with higher fracture resistance in the in vitro test exhibited lower tooth deformation in the in silico analysis, as can be seen in Table 3. Tooth deformation in EI was 9.5% greater than in RO and 27% greater than in EO, although the latter difference was not observable in the fracture resistance test. Fig. 7 visualizes the tooth formation in the different groups.

A possible correlation was observed between the frequency of repairability (in vitro) and tooth deformation (in silico). Groups with higher frequencies of repairability (UI and EI) were associated with increased tooth deformation, as displayed in Fig. 6. The Pearson's r was 0.397 indicating a moderate correlation, however it was not statistically significant. Due to the restricted amount of data, visual analysis is suitable (Schober et al., 2018). Trendlines visualize the moderate correlation. Greater tooth deformation in the coronal area resulted in reduced stress concentration on the root, leading to more favorable failures.

4. Discussion

This study tested whether different preparation designs could improve the fracture strength and failure behavior of molars restored with lithium disilicate inlays and overlays in conjunction with IDS after thermomechanical fatigue. A finite element analysis was used to better understand the failure patterns. To our knowledge, this was not previously investigated.

The first null hypothesis, stating that there would be no difference in the propagation of microcracks, could not be rejected as the Fisher exact test reported no apparent influence of the preparation design on an increase in microcracks. This is in consensus with another study, in which minimal influence of polymerization shrinkage in indirect restorations was observed (Batalha-Silva et al., 2013; Magne and Milani, 2023). This

Table 3
Descriptives of tooth deformation (FEA) and fracture strength of the different preparations groups: mean, minimum, maximum, and 95% confidence interval. UI: undermined inlay, EI: extended inlay, RO: restricted overlay, EO: extended overlay. Different superscript letters indicate significant differences.

	n	Fracture strength (N)					Tooth deformation (x10^{-4} mm)
		Mean ± SD	Minimum	Maximum	95% Confidence Interval for Mean		
					Lower Bound	Upper Bound	
UI	16	1048,88 ± 490,46[a,b]	517,71	2531,04	787,54	1310,23	98
EI	16	929,05 ± 328,62[b]	568,10	1850,41	753,94	1104,16	94
RO	16	1271,95 ± 402,43[a]	498,52	2186,89	1049,09	1494,81	85
EO	16	1200,28 ± 538,27[a,b]	488,16	2726,05	902,19	1498,36	68

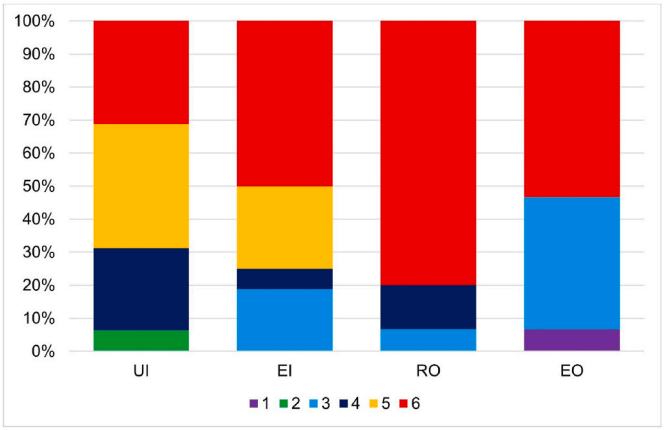

Fig. 4. Frequencies of failure modes after load to failure: 1) Dislodgement of restoration; 2) Fracture of enamel and dentin; 3) Fracture of the restoration; 4) Fracture of the restoration and enamel; 5) Fracture of the restoration, enamel, and dentin; 6) Root fracture. UI = undermined inlay, EI = extended inlay, RO = restricted overlay, EO = extended overlay.

Fig. 5. Representative examples of failure modes after load to failure test: 1) Dislodgement of the restoration; 2) Fracture of enamel and dentin; 3) Fracture of the restoration; 4) Fracture of the restoration and enamel; 5) Fracture of the restoration, enamel, and dentin; 6) Root fracture.

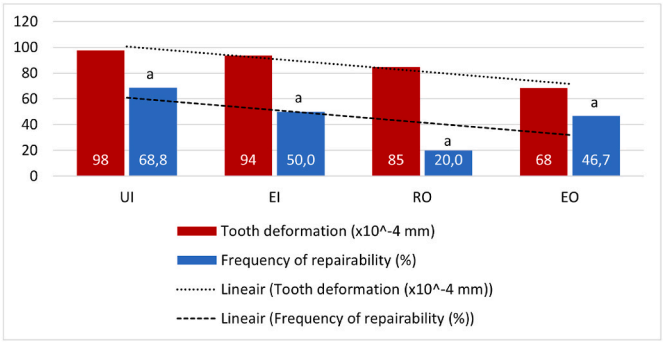

Fig. 6. Frequencies of repairability in conjunction with tooth deformation. Same letter indicates no statistical differences found among groups for repairability. UI: undermined inlay, EI: extended inlay, RO: restricted overlay, EO: extended overlay. Tooth deformation: UI: 98 × 10^{-4} mm, EI: 94 × 10^{-4} mm, RO: 85 × 10^{-4} mm, EO: 68 × 10^{-4} mm. Repairability: UI: 68.8% repairable, EI: 50% repairable, RO: 20% repairable, EO: 46.7% repairable. Trendlines visualize the possible positive correlation between tooth deformation and reparability.

was expected as only the flowable in the undermined inlay and the thin layer of pre-heated composite used for luting the restorations induced polymerization stresses. The second hypothesis, stating that there would be no statistically significant effect of preparation design on the fracture strength, could be rejected. The restricted overlay obtained statistically significant higher fracture strength than the extended inlay. However the test results were marginally statistically significant. The spread of the standard deviation could influence the significance and could have led to no statistically significant differences between the other groups. These results were in consensus with a study which reported higher fracture strength in teeth restored with lithium disilicate onlay restorations (Bresser et al., 2020; Hofsteenge et al., 2021; Magne et al., 2012; Wafaie et al., 2018). However, Hofsteenge et al. (2020) demonstrated no statistically significant apparent difference in fracture strength between inlays and onlays with IDS (Hofsteenge et al., 2020). The fracture strength of all the groups were lower in comparable to that study, which could be explained by the size of the molars used in this study, as 80–90% of the included molars were smaller than the average first mandibular molar (Nelson, 2015). Axial masticatory forces applied in humans are presumed to deviate between 40 and 240 N (Gibbs et al., 1981; Morneburg and Pröschel, 2002). Moreover, in addition to these axial forces, there are also less studied lateral shear forces during mastication, which are reported to be lower than axial forces (Koolstra et al., 1988; Koolstra and van Eijden, 1992). The maximal axial bite forces range from approximately 600 N for females to 900 N for males (Varga et al., 2011). The mean obtained forces to fracture in this study, with a loading under a 30° angle, ranged 929–1200 N and would therefore be sufficient to withstand occlusal during functional occlusal loads. A clinical study lithium disilicate restorations with preparation design and IDS as in this study shows excellent survival and success rates, respectively 99.6% and 98.6%, after a mean follow-up of 5 years.[37] Considering failure mode, the third null hypothesis stating that there would be no difference in failure mode between the groups could be rejected. The Fisher exact test revealed that the undermined inlay group exhibited a different failure pattern than the extended inlay and restricted overlay groups. Root fractures were the predominant failure pattern in restricted overlays, while undermined inlays gave a variety of failure modes. The more destructive failure pattern for onlays and overlays was also observed in other in vitro studies utilizing IDS (Hofsteenge et al., 2020, 2021; Bresser et al., 2020). The forces obtained in this study were higher than masticatory forces, which could explain why these destructive failures of ceramic restorations were not seen in clinical studies with overlays (Beier, 2012). However, a non-significant difference has been observed in terms of reparability. As a result, the

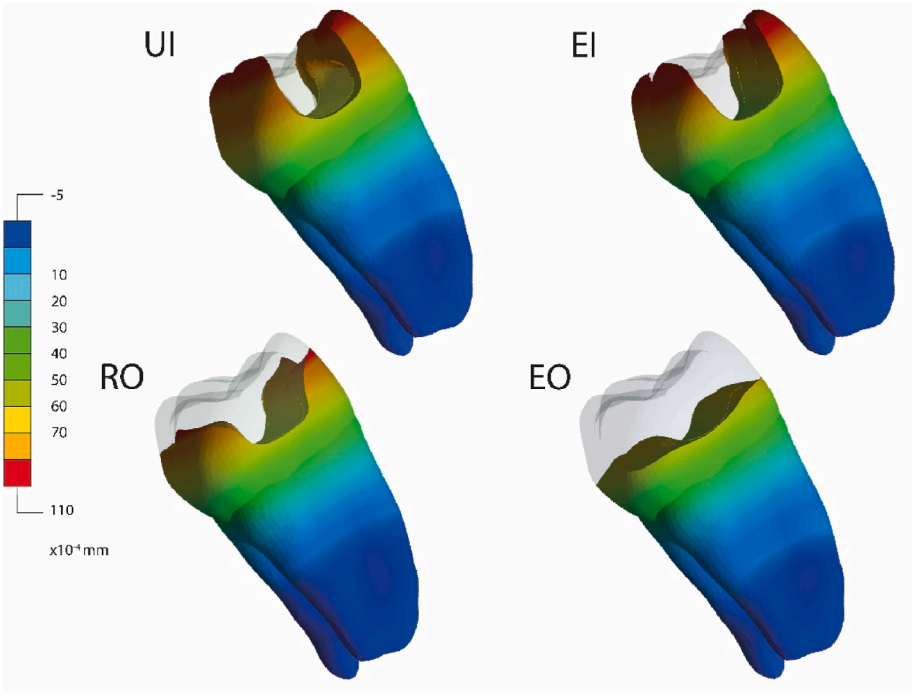

Fig. 7. Visualization of tooth deformation in the experimental preparation groups loaded at a 30° angle to the tooth axis. Tooth deformation in $x10^{-4}$ mm. UI: undermined inlay, EI: extended inlay, RO: restricted onlay, EO: extended onlay.

fourth null hypothesis, which states that there would be no statistically significant difference in repairability between the preparation groups could not be rejected. While repairability differences ranged from 68.8% for the undermined inlay restorations to 20% for the restricted overlay groups, indicating a higher occurrence of irreparable failures in the restricted overlay group, these differences were not supported by statistically significant analytical results. These findings were not in consensus with previous research, which observed more irreparable failures in onlay groups (Hofsteenge et al., 2020; Magne and Milani, 2023). Considering the fifth hypothesis, the results from the finite element analysis demonstrated a difference in tooth deformation between in silico models, which could be correlated to the fracture strength and repairability of the in vitro groups. Therefore the null hypothesis could not be accepted. The present study showed decreasing tooth deformation with the application of an overlay preparation. The extensive overlay presented lower tooth deformation than the restricted overlay, which was in consensus with a previous study (Lin et al., 2008).

There are some limitations to this laboratory study. Load to failure was used as the test method in this study to determine the fracture strength of the restored specimens. The clinical loading is different, as teeth experience repeated, minor forces that can ultimately cause dental restorations or teeth to fail. Therefore, failures in this study were consequently more destructive and less frequently repairable in comparison to the clinical situation, which is a limitation of such studies. Clinical studies on lithium disilicate partial restorations did not report fractures extending into the root, but if there were fractures, they were predominantly in the ceramic restorative material (Van den Breemer et al., 2021; Malament et al., 2021). Caution should be taken when extrapolating the results of this in vitro study to the clinical scenario. The use of cyclic isometric loading, which is more comparable to the clinical situation, could be more suitable (Magne et al., 2016). Another limitation of this study could be the limited number of specimens per group. Despite notable differences in repairability, these did not reach statistical significance, suggesting that larger sample sizes should be considered in future studies. In addition, there is a wide variety of storage media, including saliva, water, or disinfectant, as well as storage temperatures that range from low (4 °C) to oral environment temperatures (37 °C). In future studies, there should be a greater consensus on standardized storage conditions. Doubts may arise regarding the suitability of using a light-cured composite for delivering thick lithium disilicate restorations. Nonetheless, previous studies have demonstrated the successful conversion of composite material beneath a considerable layer of lithium disilicate (Gregor et al., 2014; de Kuijper et al., 2021). To ensure thorough conversion, the choice was made to use high translucency (HT) lithium disilicate blocks for this specific study. Numerous laboratory and clinical investigations have reported favorable outcomes with this delivery approach (Hofsteenge et al., 2020; Gresnigt et al., 2013; van den Breemer et al., 2019a; van den Breemer et al., 2019b; Gresnigt et al., 2019; Bresser et al., 2019; Kameyama et al., 2015). All restorations seem able to withstand adequate forces for clinical use, as mentioned earlier. Future studies should focus more on patient-associated and practitioner-associated variables to determine their influence on the longevity of lithium disilicate partial restorations on weakened molars.

Overall, it appears that extension of the preparation for the prevention of tooth fracture is not necessarily beneficial and should be questioned, even in compromised molars. There was no statistically significant difference in fracture strength between undermined inlays and restricted and extended overlays. There is no need for cusp coverage, and undermined enamel could be preserved before restoration. The FEA results, which show lower root stresses in inlay preparations combined with more favorable failure patterns, argue for tissue preservation. Undermined cusps could be reconstructed using flowable composite to enable indirect restoration fabrication. Therefore, a minimally invasive preparation, which only removes decayed tissue, could be used in daily practice based on the findings from the present study.

5. Conclusions

From this study, the following could be concluded.

1) Preparation design influences the fracture strength of compromised molars restored with lithium disilicate inlays and overlays. In

particular, a significantly lower fracture strength for extended inlays was observed.
2) The failure pattern of lithium disilicate overlays was more destructive than that of undermined and extended inlays.
3) The finite element analysis showed more tooth deformation in the inlay restorations, with lower forces in the roots, which presumably leads to less destructive fractures.
4) Given the more destructive fracture pattern in overlays, the results suggest that the undermined inlay preparation design is a viable option for restoring weakened molars.

CRediT authorship contribution statement

Jelte W. Hofsteenge: Writing – original draft, Visualization, Methodology, Investigation, Formal analysis, Conceptualization. **Marco Aurelio Carvalho:** Writing – review & editing, Writing – original draft, Visualization, Software, Methodology, Formal analysis, Conceptualization. **Pauline M. Borghans:** Writing – original draft, Investigation, Formal analysis. **Marco S. Cune:** Writing – review & editing, Supervision, Resources, Conceptualization. **Mutlu Özcan:** Writing – review & editing, Supervision, Conceptualization. **Pascal Magne:** Writing – review & editing, Methodology, Conceptualization. **Marco M.M. Gresnigt:** Writing – review & editing, Supervision, Resources, Methodology, Conceptualization.

Declaration of competing interest

The authors declare that they have no known competing financial interests or personal relationships that could have appeared to influence the work reported in this paper.

Data availability

Data will be made available on request.

Acknowledgements

The authors extend their gratitude to Douwe Postma for his help with the statistical analysis. The authors acknowledge Ivoclar Vivadent, Liechtenstein for supplying some of the materials used in this study.

Appendix A. Supplementary data

Supplementary data to this article can be found online at https://doi.org/10.1016/j.jmbbm.2023.106096.

References

Abduo, J., Sambrook, R.J., 2018. Longevity of ceramic onlays: a systematic review. J. Esthetic Restor. Dent. 30 (3), 193–215.
Alassar, R.M., Samy, A.M., Abdel-Rahman, F.M., 2021. Effect of cavity design and material type on fracture resistance and failure pattern of molars restored by computer-aided design/computer-aided manufacturing inlays/onlays. Dent. Res. J. 18, 14.
Amesti-Garaizabal, Agustín-Panadero, Verdejo-Solá, Fons-Font, Fernández-Estevan, Montiel-Company, et al., 2019. Fracture resistance of partial indirect restorations made with CAD/CAM Technology. A systematic review and meta-analysis. J. Clin. Med. 8 (11), 1932.
Ausiello, P.P., Ciaramella, S., Lanzotti, A., Ventre, M., Borges, A.L., Tribst, J.P., et al., 2019. Mechanical behavior of Class I cavities restored by different material combinations under loading and polymerization shrinkage stress. A 3D-FEA study. Am. J. Dent. 32 (2), 55–60.
Batalha-Silva, S., De Andrada, M.A.C., Maia, H.P., Magne, P., 2013. Fatigue resistance and crack propensity of large MOD composite resin restorations: direct versus CAD/CAM inlays. Dent. Mater. 29 (3), 324–331.
Beier, U.S., 2012. Clinical long-term evaluation and failure characteristics of 1,335 all-ceramic restorations. J. Prosthet. Dent 107 (4), 238.
van den Breemer, C.R.G., Özcan, M., Cune, M.S., van der Giezen, R., Kerdijk, W., Gresnigt, M.M.M., 2017. Effect of immediate dentine sealing on the fracture strength of lithium disilicate and multiphase resin composite inlay restorations. J. Mech. Behav. Biomed. Mater. 72, 102–109.
van den Breemer, C.R.G., Cune, M.S., Özcan, M., Naves, L.Z., Kerdijk, W., Gresnigt, M.M.M., 2019a. Randomized clinical trial on the survival of lithium disilicate posterior partial restorations bonded using immediate or delayed dentin sealing after 3 years of function. J. Dent. 85, 1–10 (February). https://linkinghub.elsevier.com/retrieve/pii/S0300571218302379.
van den Breemer, C., Gresnigt, M., Özcan, M., Kerdijk, W., Cune, M., 2019b. Prospective randomized clinical trial on the survival of lithium disilicate posterior partial crowns bonded using immediate or delayed dentin sealing: short-term results on tooth sensitivity and patient satisfaction. Operat. Dent. 45 (5), E212–E222.
Van den Breemer, C.R.G., Buijs, G.J., Cune, M.S., Özcan, M., Kerdijk, W., Van der Made, S., et al., 2021. Prospective clinical evaluation of 765 partial glass-ceramic posterior restorations luted using photo-polymerized resin composite in conjunction with immediate dentin sealing. Clin. Oral Invest. 25 (3), 1463–1473.
Bresser, R.A., Gerdolle, D., van den Heijkant, I.A., Sluiter-Pouwels, L.M.A., Cune, M.S., Gresnigt, M.M.M., 2019. Up to 12 years clinical evaluation of 197 partial indirect restorations with deep margin elevation in the posterior region. J. Dent. 91, 103227.
Bresser, R.A., van de Geer, L., Gerdolle, D., Schepke, U., Cune, M.S., Gresnigt, M.M.M., 2020. Influence of Deep Margin Elevation and preparation design on the fracture strength of indirectly restored molars. J. Mech. Behav. Biomed. Mater. 110.
Camargos, G.D.V., Lazari-Carvalho, P.C., Carvalho, MA de, Castro, M.B., Neris, N.W., Del Bel Cury, A.A., 2020. 3D finite element model based on CT images of tooth: a simplified method of modeling. Braz. J. Oral Sci. 19, e208910.
Dejak, B., Młotkowski, A., 2015. A comparison of stresses in molar teeth restored with inlays and direct restorations, including polymerization shrinkage of composite resin and tooth loading during mastication. Dent. Mater. 31 (3), e77–e87.
Faul, F., Erdfelder, E., Lang, A.G., Buchner, A.G., 2007. *Power 3: a flexible statistical power analysis program for the social, behavioral, and biomedical sciences. Behav. Res. Methods 39 (2), 175–191.
Gibbs, C.H., Mahan, P.E., Lundeen, H.C., Brehnan, K., Walsh, E.K., Holbrook, W.B., 1981. Occlusal forces during chewing and swallowing as measured by sound transmission. J. Prosthet. Dent 46 (4), 443–449.
Gregor, L., Bouillaguet, S., Onisor, I., Ardu, S., Krejci, I., Rocca, G.T., 2014. Microhardness of light- and dual-polymerizable luting resins polymerized through 7.5-mm-thick endocrowns. J. Prosthet. Dent 112 (4), 942–948.
Gresnigt, M.M.M., Kalk, W., Özcan, M., 2013. Clinical longevity of ceramic laminate veneers bonded to teeth with and without existing composite restorations up to 40 months. Clin. Oral Invest 17 (3), 823–832.
Gresnigt, M.M.M., Cune, M.S., Schuitemaker, J., van der Made, S.A.M., Meisberger, E.W., Magne, P., et al., 2019. Performance of ceramic laminate veneers with immediate dentine sealing: an 11 year prospective clinical trial. Dent. Mater. 35 (7), 1042–1052.
Hofsteenge, J.W., Hogeveen, F., Cune, M.S., Gresnigt, M.M.M., 2020. Effect of immediate dentine sealing on the aging and fracture strength of lithium disilicate inlays and overlays. J. Mech. Behav. Biomed. Mater. 110 (April), 103906.
Hofsteenge, J.W., van den Heijkant, I.A., Cune, M.S., Bazos, P.K., van der Made, S., Kerdijk, W., et al., 2021. Influence of preparation design and restorative material on fatigue and fracture strength of restored maxillary premolars. Operat. Dent. 46 (2), E68–E79.
Kameyama, A., Bonroy, K., Elsen, C., Lührs, A.K., Suyama, Y., Peumans, M., et al., 2015. Luting of CAD/CAM ceramic inlays: direct composite versus dual-cure luting cement. Bio Med. Mater. Eng. 25 (3), 279–288.
Koolstra, J.H., van Eijden, T.M.G.J., 1992. Application and validation of a three-dimensional mathematical model of the human masticatory system in vivo. J. Biomech. 25 (2), 175–187.
Koolstra, J.H., van Eijden, T.M.G.J., Weijs, W.A., Naeije, M., 1988. A three-dimensional mathematical model of the human masticatory system predicting maximum possible bite forces. J. Biomech. 21 (7), 563–576.
de Kuijper, M.C.F.M., Ong, Y., Gerritsen, T., Cune, M.S., Gresnigt, M.M.M., 2021. Influence of the ceramic translucency on the relative degree of conversion of a direct composite and dual-curing resin cement through lithium disilicate onlays and endocrowns. J. Mech. Behav. Biomed. Mater. 122.
Kuijs, R.H., Roeters, F.J.M., Burgersdijk, R.C.W., Fennis, W.M.M., Kreulen, C.M., Creugers, N.H.J., 2006. A randomized clinical trial of cusp-replacing resin composite restorations: efficiency and short-term effectiveness. Int. J. Prosthodont. (IJP) 19 (4), 349–354.
Lan, T.H., Pan, C.Y., Lee, H.E., Huang, H.L., Wang, C.H., 2010. Bone stress analysis of various angulations of mesiodistal implants with splinted crowns in the posterior mandible: a three-dimensional finite element study. Int. J. Oral Maxillofac. Implants 25 (4), 763–770.
Lin, C.L., Chang, Y.H., Liu, P.R., 2008. Multi-factorial analysis of a cusp-replacing adhesive premolar restoration: a finite element study. J. Dent. 36 (3), 194–203.
Magne, P., Milani, T., 2023. Short-fiber reinforced MOD restorations of molars with severely undermined cusps. J. Adhesive Dent. 25 (1), 99–106.
Magne, P., Boff, L.L., Oderich, E., Cardoso, A.C., 2012. Computer-aided-design/computer-assisted-manufactured adhesive restoration of molars with a compromised cusp: effect of fiber-reinforced immediate dentin sealing and cusp overlap on fatigue strength. J. Esthetic Restor. Dent. 24 (2), 135–146.
Magne, P., Goldberg, J., Edelhoff, D., Güth, J.F., 2016. Composite resin core buildups with and without post for the restoration of endodontically treated molars without ferrule. Operat. Dent. 41 (1), 64–75.
Malament, K.A., Margvelashvili-Malament, M., Natto, Z.S., Thompson, V., Rekow, D., Att, W., 2021. 10.9-year survival of pressed acid etched monolithic e.max lithium disilicate glass-ceramic partial coverage restorations: performance and outcomes as a function of tooth position, age, sex, and the type of partial coverage restoration (inlay or onlay). J. Prosthet. Dent 126 (4), 523–532.

Manhart, J., Chen, H., Hamm, G., Hickel, R., 2004. Buonocore Memorial Lecture. Review of the clinical survival of direct and indirect restorations in posterior teeth of the permanent dentition. Operat. Dent. 29 (5), 481–508.
Mondelli, J., Sene, F., Ramos, R.P., Benetti, A.R., 2007. Tooth structure and fracture strength of cavities. Braz. Dent. J. 18 (2), 134–138.
Morneburg, T.R., Pröschel, P.A., 2002. Measurement of masticatory forces and implant loads: a methodologic clinical study. Int. J. Prosthodont. (IJP) 15 (1), 20–27.
Nelson, S., 2015. Wheeler's dental anatomy, physiology, and occlusion. J. Chem. Inf. Model. 53, 183–202.
Park, J.H., Choi, N.S., 2017. Equivalent Young's modulus of composite resin for simulation of stress during dental restoration. Dent. Mater. 33 (2), e79–e85.
Politano, G., Van Meerbeek, B., Peumans, M., 2018. Nonretentive bonded ceramic partial crowns: concept and simplified protocol for long-lasting dental restorations. J. Adhesive Dent. 20 (6), 495–510.
Qanungo, A., Aras, M.A., Chitre, V., Mysore, A., Amin, B., Daswani, S.R., 2016. Immediate dentin sealing for indirect bonded restorations. J Prosthodont Res 60 (4), 240–249.
Rita, A., Reis, J., Santos, I.C., Delgado, A.H.S., Rua, J., Proença, L., et al., 2021. Influence of silane type and application time on the bond strength to leucite reinforced ceramics. Ann. Med. 53 (Suppl. 1). S67–S67.
Rocca, G.T., Rizcalla, N., Krejci, I., Dietschi, D., 2015. Evidence-based concepts and procedures for bonded inlays and onlays. Part II. Guidelines for cavity preparation and restoration fabrication. Int J Esthet Dent 10 (3), 392–413.
Rodrigues, M. de P., Soares, P.B.F., Gomes, M.A.B., Pereira, R.A., Tantbirojn, D., Versluis, A., et al., 2020. Direct resin composite restoration of endodontically-treated permanent molars in adolescents: bite force and patient-specific finite element analysis. J. Appl. Oral Sci. 28, e20190544.
Schober, P., Boer, C., Schwarte, L.A., 2018. Correlation coefficients: appropriate use and interpretation. Anesth. Analg. 126 (5), 1763–1768.
Trindade, F.Z., Valandro, L.F., de Jager, N., Bottino, M.A., Kleverlaan, C.J., 2018. Elastic properties of lithium disilicate versus feldspathic inlays: effect on the bonding by 3D finite element analysis. J. Prosthodont. 27 (8), 741–747.
Varga, S., Spalj, S., Lapter Varga, M., Anic Milosevic, S., Mestrovic, S., Slaj, M., 2011. Maximum voluntary molar bite force in subjects with normal occlusion. Eur. J. Orthod. 33 (4), 427–433.
Wafaie, R.A., Ibrahim Ali, A., Mahmoud, S.H., 2018. Fracture resistance of prepared premolars restored with bonded new lab composite and all-ceramic inlay/onlay restorations: laboratory study. J. Esthetic Restor. Dent. 30 (3), 229–239.
Yamanel, K., Çağlar, A., Gülşahi, K., Özden, U.A., 2009. Effects of different ceramic and composite materials on stress distribution in inlay and onlay cavities: 3-D finite element analysis. Dent. Mater. J. 28 (6), 661–670.
Yoon, H.I., Sohn, P.J., Jin, S., Elani, H., Lee, S.J., 2019. Fracture resistance of CAD/CAM-Fabricated lithium disilicate MOD inlays and onlays with various cavity preparation designs. J. Prosthodont. 28 (2), e524–e529.